Tunable Axion Plasma Haloscopes

Matthew Lawson,[1,2] Alexander J. Millar,[1,2,*] Matteo Pancaldi,[3] Edoardo Vitagliano,[4] and Frank Wilczek[1,2,5,6,7,8]

[1]*The Oskar Klein Centre for Cosmoparticle Physics, Department of Physics, Stockholm University,*
AlbaNova, 10691 Stockholm, Sweden
[2]*Nordita, KTH Royal Institute of Technology and Stockholm University, Roslagstullsbacken 23, 10691 Stockholm, Sweden*
[3]*Department of Physics, Stockholm University, AlbaNova, 10691 Stockholm, Sweden*
[4]*Max-Planck-Institut für Physik (Werner-Heisenberg-Institut), Föhringer Ring 6, 80805 München, Germany*
[5]*Center for Theoretical Physics, Massachusetts Institute of Technology, Cambridge, Massachusetts 02139, USA*
[6]*T. D. Lee Institute, Shanghai 200240, China*
[7]*Wilczek Quantum Center, Department of Physics and Astronomy, Shanghai Jiao Tong University, Shanghai 200240, China*
[8]*Department of Physics and Origins Project, Arizona State University, Tempe, Arizona 25287, USA*

We propose a new strategy for searching for dark matter axions using tunable cryogenic plasmas. Unlike current experiments, which repair the mismatch between axion and photon masses by breaking translational invariance (cavity and dielectric haloscopes), a plasma haloscope enables resonant conversion by matching the axion mass to a plasma frequency. A key advantage is that the plasma frequency is unrelated to the physical size of the device, allowing large conversion volumes. We identify wire metamaterials as a promising candidate plasma, wherein the plasma frequency can be tuned by varying the interwire spacing. For realistic experimental sizes, we estimate competitive sensitivity for axion masses of 35–400 μeV, at least.

Introduction.—One of the most pressing problems in cosmology is the composition of dark matter (DM). Recently, the axion has been pushed towards the limelight as a DM candidate. Consequently, there is increasing urgency in developing strategies to search for this elusive particle. The axion was introduced via the Peccei-Quinn (PQ) mechanism to solve the puzzling absence of significant *CP* violation in quantum chromodynamics (QCD): the strong *CP* problem. The PQ mechanism essentially replaces the *CP* violating phase θ with a field which has a potential minimum at $\theta = 0$ (the axion) [1–3]. Here, the strong *CP* problem is solved dynamically, with the axion relaxing to the bottom of its potential over cosmological time scales.

Residual oscillations of the axion field, while very small, remain until the present day and act as cold dark matter [4]. Depending on the exact cosmological history, a wide range of axion masses m_a can provide the correct abundance of dark matter, from 10^{-6}–10^3 μeV. Cosmology allows us to consider two broad scenarios. The axion itself is a pseudo-Goldstone boson generated by the breaking of the PQ symmetry; whether or not this symmetry is restored after inflation sets the initial conditions for the axion field. If the symmetry is restored after inflation, in each causally separated region of space the initial angle θ_i adopts a different value. As our observable Universe would consist of many such patches, we live in an "averaged" Universe where the dark matter abundance is simply set by m_a. In addition, due to large inhomogeneities in the axion field, topological defects such as strings and domain walls may form. These topological defects lead to difficulty in calculating the preferred axion mass [5,6], though recent calculations suggest $m_a = 25.2 \pm 11.0$ μeV [7,8]. Note, however, that large log factors are still poorly understood and may significantly change this prediction [9,10].

In contrast, if the PQ symmetry is not restored after inflation, then the same θ_i exists throughout the observable Universe. The exact value cannot be predicted, though often $\theta_i = \mathcal{O}(1)$ is considered "natural," giving 10^{-1} μeV $\lesssim m_a \lesssim 100$ μeV.

Searches based on cavity resonators in strong magnetic fields [11] like ADMX [12], HAYSTAC [13], CULTASK [14], KLASH [15], or ORGAN [16] are optimal for $m_a \lesssim 10$ μeV. Significantly lower values of m_a can be explored by *LC* circuits [17,18] or nuclear magnetic resonance techniques like CASPER [19]. Recently, dielectric haloscopes [20,21] were introduced to tackle the higher mass parameter space ($m_a \gtrsim 40$ μeV). However, the technique is still under development. Similarly, the high mass performance of cavity haloscopes relies on unproven

techniques such as combining large numbers of cavities [16,22,23].

In this Letter, we consider the coupling of the axion to bulk plasmons, rather than photons. The resonant mixing of axions with plasmons was first noted in [24–26], but it was generally ignored until recently [27–29]. Concurrent with this work, the idea of plasma-shining-through-wall has been introduced [30]. Here, we consider the mixing of axions to tunable plasmas which can operate at cryogenic temperatures, thus, leading to the first practical proposal to search for axions using axion-plasmon resonance.

One key advantage to such a scheme, as we will demonstrate, is that the resonant frequency of the experiment is decoupled from its physical dimensions, side-stepping one of the main difficulties of building high frequency cavity haloscopes. Thus, we expect a significant increase in the generated signal at high frequencies, even for less resonant setups.

Axion-Plasmon resonance in finite media.—Despite axion-photon mixing being noted almost immediately after the introduction of the axion, the concomitant axion-plasmon mixing has been generally neglected. Throughout this Letter, we will use natural units with the Lorentz-Heaviside convention. The axion's interaction with electrodynamics is described by a term

$$\mathcal{L} \supset -\frac{g_{a\gamma}}{4} F_{\mu\nu} \tilde{F}^{\mu\nu} a, \qquad (1)$$

with the coupling strength between axions and photons governed by the dimensionful constant $g_{a\gamma}$. The axion's mass and couplings are given by the decay constant f_a, with $m_a f_a \sim m_\pi f_\pi$ and $g_{a\gamma} = -(\alpha/2\pi f_a)C_{a\gamma}$, with $C_{a\gamma}$ an $\mathcal{O}(1)$ model dependent number and α the fine structure constant. We use $F_{\mu\nu}$ to denote the electromagnetic field-strength tensor, with the dual tensor $\tilde{F}^{\mu\nu} = \frac{1}{2}\varepsilon^{\mu\nu\alpha\beta}F_{\alpha\beta}$. Axion dark matter is extremely cold ($v \sim 10^{-3}$), giving a correspondingly large de Broglie wavelength $\lambda_{dB} = 2\pi/m_a v_a$. Thus, the axion acts essentially as a spatially constant classical field oscillating with a frequency $\omega_a = m_a$, given by $a(t) = a_0 e^{-i\omega_a t}$. In the presence of an external magnetic field $\mathbf{B}_e$, the only modification to Maxwell's equations to lowest order in $g_{a\gamma}$ is in Ampère's law. Because of the smallness of the coupling we will only consider linear order effects in $g_{a\gamma}$.

$$\mathbf{\nabla}\times\mathbf{H} - \dot{\mathbf{D}} = g_{a\gamma}\mathbf{B}_e\dot{a}. \qquad (2)$$

The primary effect of the axion is to act like an oscillating current, driving the system at ω_a. Alternatively, one can think of $\mathbf{B}_e$ inducing a mixing between the axion and photon. Because of conservation of momentum and energy, the massive axion cannot convert to a massless photon in an infinite space. In order to allow conversion between the two particles, one must either overcome the difference in

dispersion relation or break translation invariance. Cavity and dielectric haloscopes do the latter by introducing structure on the scale of the Compton wavelength, allowing for the momentum mismatch to be satisfied. However, it is also possible to match dispersion relations by tuning the mass of the photon (plasma frequency) to that of the axion. In this case, one does not need to break translation invariance, allowing for systems to be much larger than the Compton wavelength.

Infinite plasma: Previously, analysis of axion-plasmon mixing has been limited to the case of an infinite homogenous medium. In this case, Maxwell's equations become particularly simple; if we consider an E field in a linear medium with dielectric constant ϵ, we see that

$$\mathbf{E} = -\frac{g_{a\gamma}\mathbf{B}_e a}{\epsilon} = -g_{a\gamma}\mathbf{B}_e a\left(1 - \frac{\omega_p^2}{\omega_a^2 - i\omega_a\Gamma}\right)^{-1}, \quad (3)$$

where, in the last equality, we have introduced a Drude model for the dielectric constant. The plasma frequency is denoted by ω_p, with Γ being the small damping rate which sets the plasmon lifetime. In the limit $\mathrm{Re}(\epsilon) \to 0$, a resonance occurs, corresponding to matching the axion frequency ω_a to the plasma frequency ω_p. Importantly, the resonant frequency is a property of the medium, rather than being a function of the size of the system, as is the case for cavity haloscopes.

Plasma cylinder: As any experiment must be finite in extent, we will now turn our attention to bounded plasmas. In particular, we take the plasma to be bounded inside a conductive cylinder. Similar cases are often considered under the label of "plasma waveguides," which permits a similar analysis [31].

The length of the cylinder is not actually relevant to the E- and B-field distributions, as any mismatch at the end caps is simply met by surface charges given by $(\mathbf{D}_2 - \mathbf{D}_1) \cdot \mathbf{n}_{12} = \sigma_s$. We choose cylindrical coordinates (r, ϕ, z) and take $\mathbf{B}_e$ to be in the z direction, i.e., $\mathbf{B}_e = B_e\hat{\mathbf{z}}$. As the axion is taken to be spatially constant, translational symmetry in the z direction implies that all fields are similarly constant in the z direction. In anticipation of a thin wire metamaterial, we will assume that the medium only has a nonunity dielectric constant ϵ_z in one direction, aligned with the cylinder. More generally, the strong applied magnetic field will ensure a highly anisotropic medium response.

The cylindrical symmetry allows us to directly solve the axion-Maxwell equations at a radius r inside a cylinder of total radius R, giving

$$\mathbf{E}_z = -\frac{ag_{a\gamma}B_e}{\epsilon_z} + \frac{ag_{a\gamma}B_e}{\epsilon_z}\frac{J_0(\sqrt{\epsilon_z}r\omega)}{J_0(\sqrt{\epsilon_z}R\omega)}, \qquad (4a)$$

$$\mathbf{B} = -\frac{ag_{a\gamma}B_e}{\sqrt{\epsilon_z}}\frac{J_1(\sqrt{\epsilon_z}r\omega)}{J_0(\sqrt{\epsilon_z}R\omega)}\hat{\boldsymbol{\phi}}, \qquad (4b)$$
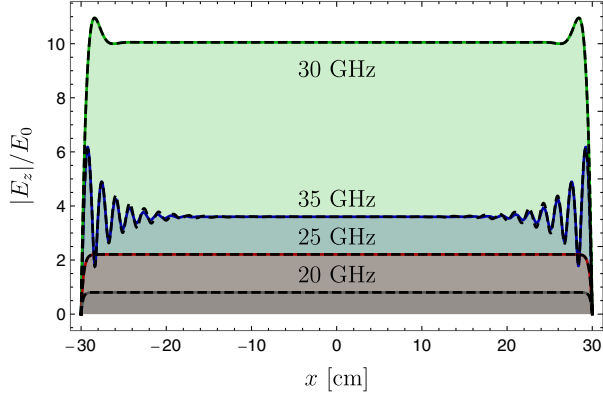
FIG. 1.   Analytic and numerical calculation of E field as a function of radius in an infinite, 30 cm radius cylinder of plasma contained inside conductive walls. We have defined $E_0 = g_{a\gamma}B_e a_0$. The plasma is characterized by $\omega_p = 30$ GHz and $\Gamma = 10^{-1} \times \omega_p$, with axion frequencies $\omega = 20, 25, 30$, and 35 GHz plotted. The colored lines indicated the analytical calculation and the black dashed lines the numerical. Numerical calculations were performed in COMSOL for a 2.7m long cylinder.

where J_i is a Bessel function of the first kind. To unpack these expressions, note that we are interested in bulk plasmons, where $\mathrm{Re}(\epsilon_z) = 0$. As $J_0(0) = 1$, behavior in the center of the medium is dominated by $J_0(\sqrt{\epsilon_z}R\omega)$. When $R \gtrsim \pi/\sqrt{\epsilon_z}\omega$ the second term in equation (4a) and only term in (4b) can be neglected at the center. In other words, a sufficiently large medium has a bulk that behaves exactly the same as in the infinite medium case. This relationship gives us a minimum size for a given haloscope. Note that, unlike cavity or dielectric haloscopes, the enhancement of the E field is not related to boundary conditions: the same would occur for an infinite medium, or one surrounded by vacuum.

To see these examples in action, in Fig. 1 we plot the electric field profile in a 30 cm radius cylinder, with $\omega_p = 30$ GHz and $\Gamma = 10^{-1} \times \omega_p$. These are fairly conservative parameters, choosing a very lossy plasma. As expected, we see a large homogeneous region in the center of the cylinder, with the edges having a small spike before rapidly vanishing at the edges. We test our analytic calculations by comparison to numerical calculations performed in COMSOL [32]. The analytic and numerical calculations are essentially identical, showing a resonance when the axion and plasma frequencies match.

Wire metamaterials.—In order to search for axions, we require materials that can be operated at cryogenic temperatures and have a tunable plasma frequency corresponding to the expected axion mass ($m_a \lesssim 60$ meV) [33,34]. Several possibilities exist, including electron-poor semiconductors, field effect transistors, and Josephson junctions, which can often be tuned nonmechanically [35–37]. As a prototypical example, we will, instead, focus on thin wire metamaterials [38]. One of the earliest proposed

metamaterials, a volume filled with thin wires keeps many of the nice properties of metals (such as operating at cryogenic temperatures); however, the plasma frequency of the system is vastly lower. We will consider homogeneously spaced wires aligned in the z direction of radius d and spacing s. It has been shown that, as long as the wires are sufficiently thin ($\log(s/d) \gg 1$), they act as an effective medium with a dielectric constant [38,39]

$$\epsilon_z = 1 - \frac{\omega_p^2}{\omega^2 - k_z^2 + i\omega\Gamma}, \tag{5}$$

where we have added in a small loss term. As we are neglecting the axion velocity, $k_z = 0$ so we can neglect spatial dispersion and simply recover a Drude-like model.

To see that ω_p is much smaller than in a regular metal, two effects must be considered. The first is the much lower average density of electrons n_e, and the second is the mutual inductance of the wires changing the effective electron mass m_{eff}. More explicitly, these effects give [38]

$$n_e = n\frac{\pi d^2}{s^2}; \quad m_{\mathrm{eff}} = \frac{e^2\pi d^2 n}{2\pi}\log\frac{s}{d}, \tag{6}$$

where n is the density of electrons in the wires, and e the electric charge. The corresponding plasma frequency is

$$\omega_p^2 = \frac{n_e e^2}{m_{\mathrm{eff}}} = \frac{2\pi}{s^2\log(s/d)}. \tag{7}$$

We can easily see from (7) that the plasma frequency is essentially given by the spacing between the wires, meaning that, for cm scale spacings, $\omega_p = \mathcal{O}(\mathrm{GHz})$. Further, as ω_p is a function of s, by changing the spacing of the wires, it is possible to tune the plasma frequency. Thus, we anticipate thin wire structures to be an ideal candidate plasma.

Setup.—A practical experimental realization of this scheme must accommodate a few key features. First, the size and spacing of the wires must be such that the structure can be approximated as a medium, which condition obtains when $\log(s/d) \gg 1$ (that is, the diameter of the wires is much smaller than the spacing between the wires) [38]. Copper wires with diameters as small as 10 μm are commercially available, setting a soft limit of 3 mm on the interwire spacing. This corresponds to a soft upper frequency limit of 100 GHz. For higher frequencies, the volume of the plasma will also be limited by λ_{dB}. For haloscopes velocity effects start becoming noticeable for physical distances ∼20% of λ_{dB} [27,40,41].

Second, the plasma must be placed in a strong magnetic field, which limits the maximum practical diameter of the structure. Consequently, the maximum spacing between the wires is also limited. There are commercially available magnets with 7 T fields and 60 cm bore diameters, so

taking this as a conservative upper limit, and requiring at least ~300 evenly spaced wires, we find an interwire spacing of 3 cm and a corresponding lower frequency limit of 8.8 GHz.

Third, the spacing between the wires must be tunable while retaining a relatively high level of spacing homogeneity. However, tuning may be more easily realized than it seems at first glance. While, for simplicity, we have focused on isotropic wire arrays, this condition is not necessary; anisotropically spaced wires still give an isotropic effective medium [39]. As the plasma frequency comes from the mutual inductance between the wires, the medium acts isotropically as long as the wires are arranged such that each wire feels the same mutual inductance as every other wire.

Thus, one very appealing geometry for tuning the plasma frequency is a series of planes of wires, with spacing adjusted in a single direction. We leave a full investigation of such mechanics to a technical design study. Assuming a tuning system which can cover more than a few percent of the total frequency range of the experiment is realized, one could fabricate multiple inserts which could then be used for specific ranges of frequencies. Given that the overall size of the structure is largely independent of the operating frequency, such inserts could all be identical in external dimension, facilitating relatively fast swapping into and out of the magnet, electronic, and cryogenic systems. Depending on the details, such a tuning mechanism may further limit the high frequency range.

Figure 2 shows a schematic representation of the essential features of the proposed experimental realization. An external magnetic field of order 10T is applied to an
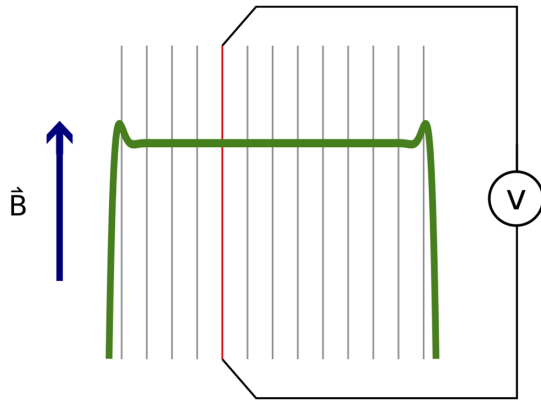

FIG. 2. A schematic representation of an experimental realization of the plasma haloscope. An array of wires with variable interwire spacing is placed in a strong uniform magnetic field. The array of wires (gray lines) acts as an effective medium with plasma frequency set (to leading order) by the wire spacing. The axion field excites a bulk plasmon in the wire metamaterial which can be detected by an antenna with the appropriate geometry (here, represented by the red line). The green curve shows the absolute value of the electric field profile within the wire metamaterial.

array of parallel wires with tunable interwire spacing. In the presence of the magnetic field, axions can induce bulk plasmons when the plasma frequency (set by the spacing) matches the axion frequency. As a result, there will be a roughly uniform axial electric field oscillating sinusoidal in time. Antennas or pickup loops inside the structure can be used to detect this oscillating electric field. An ultra-low-noise microwave amplifier then amplifies the voltage produced by the antenna. The wire assembly is electromagnetically shielded and cooled to cryogenic temperatures to reduce noise.

Projected reach.—To estimate the parameter space that could be explored by a plasma haloscope, we must first calculate the power. In general, the power that can be extracted from the plasma is related to the loss rate of the plasma. For a Drude plasma, for small Γ, the loss rate is given by $P = \Gamma U$, where U is the stored energy. This corresponds to a quality factor $Q = \omega/\Gamma$. Assuming a signal coupling efficiency factor κ, on resonance, we can write the power in a form similar to that used for cavity haloscopes [11],

$$P = \kappa \mathcal{G} V \frac{Q}{m_a} \rho_a g_{a\gamma}^2 B_e^2, \tag{8}$$

where

$$\mathcal{G} = \frac{\epsilon_z^2}{a_0^2 g_{a\gamma}^2 B_e^2 V} \frac{1}{2} \int \left(\frac{\partial(\epsilon_z \omega)}{\partial \omega} |\mathbf{E}|^2 + |\mathbf{B}|^2 \right) dV. \tag{9}$$

The local axion dark matter density is denoted ρ_a, with 0.45 GeV/cm^3 being the typical value used. In $\mathcal{G}$, we have defined a kind of "geometry factor," however, unlike a traditional cavity haloscope, $\mathcal{G} \rightarrow 1$ as $R \rightarrow \infty$. Further, as $g_{a\gamma} \propto m_a$ for the QCD axion the power actually increases at higher masses, given constant Q. Thus, the primary advantage over traditional cavity haloscopes comes from the dramatically increased measurement volume, meaning that much more energy is stored in the system. Because of this feature, plasma haloscopes will be most useful in the high frequency regime.

To calculate a scan rate, the signal to noise ratio (S/N) is given by Dicke's radiometer equation, $S/N = (P/T_{\text{sys}})\sqrt{\Delta t/\Delta \nu_a}$, where the system noise temperature is T_{sys} and the axion signal line width $\Delta \nu_a \sim 10^{-6}\nu_a$. The measurement time is denoted Δt, covering a frequency range $\sim \omega/Q$. Assuming that the tuning mechanism allows for rapid tuning and so can be neglected, it is simple to estimate the projected reach of a given experiment. Parametrizing the measurement time as $\Delta t = A\nu^p$, where A and p are independent of ν and given by Eq. (8), we can integrate Dicke's formula between some frequencies ν_1, ν_2 to get the total scanning time

$$t_{\text{scan}} = \frac{QA}{p} (\nu_2^p - \nu_1^p). \tag{10}$$

To put in some numbers, we assume a plasma with a conservative $Q = 10^2$ and $V = 0.8$ m^3 inside 10 T magnetic field. With such a conservative Q and concomitant longer measurement time, the assumption that the tuning time can be neglected should hold true. We require $S/N \geq 3$ over the full width half maximum (ω/Q). To account for the decrease in λ_{dB} at high frequencies, we assume a 60 cm bore magnet and limit the length to 30% of λ_{dB}. As shown in Fig. 3, with quantum limited detection ($T_{\text{sys}} = m_a$), the axion parameter space 35–400 μeV could be explored down to Dine–Fischler–Srednicki–Zhitnitsky [42,43] ($|C_{a\gamma}| = 0.746$) in 6 years. We have assumed that the readout system is critically coupled, i.e., $\kappa = 0.5$.

Such a detection scheme is more easily reached at low masses, where Josephson parametric amplifiers operating with a dilution refrigerator have been shown to achieve near quantum limited detection [44]. With a more modest detection system, such as a commercially available high electron mobility transistor operating in liquid helium ($T_{\text{sys}} \sim 5$ K) the higher mass range 100–160 μeV could be explored in a similar time frame (4 years). Such a scan would be complementary to the initial stages of MADMAX [20]. Above 40 GHz, new detection technology will be required regardless of the specific axion detection mechanism [52].

Because of similar design limitations, thin wire metamaterials seem most optimal in a similar parameter space as
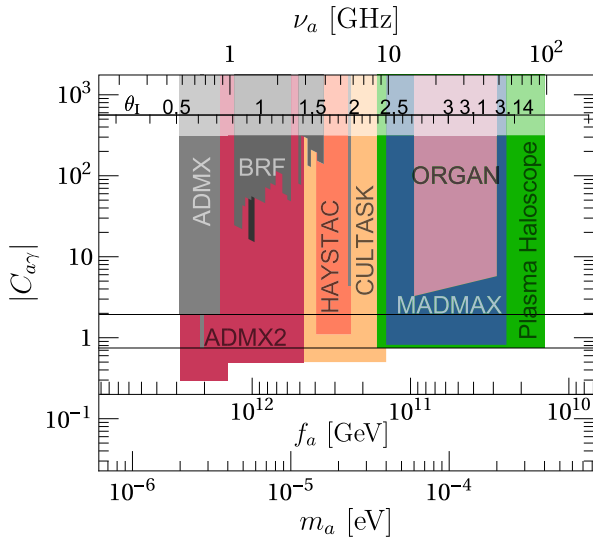

FIG. 3. In green, we show the projected reach in the $\{m_a, |C_{a\gamma}|\}$ plane of a plasma with $Q = 10^2$ and $V = 0.8$ m^3 inside 10 T magnetic field. We assume a critically coupled, quantum limited detector with a six year measurement time. The black lines bracket the traditional axion model band, $0.746 < |C_{a\gamma}| < 1.92$. Existing limits are displayed in gray, with colored regions corresponding to proposed experiments (red tones for cavities, blue for dielectric haloscopes) [13,14,20,44–51].

dielectric haloscopes. Which technique will be more practical at a given frequency depends strongly on the detailed design of an experiment. A particular advantage of plasma haloscopes is that a solenoidal, rather than dipole, magnet can be used, simplifying the design and cost. In addition, plasma haloscopes may be more easily extended into even higher mass parameter space, as the technique will work as long as an appropriate medium is found. As mentioned above, several candidate materials exist with the possibility of high Q and nonmechanical tuning and warrant further exploration.

Conclusion.—In this Letter, we have outlined a new axion detection technique using tunable cryogenic plasmas. By matching the axion and plasmon masses, we induce resonant conversion between the two. Unlike existing haloscope designs, axion-photon conversion is not caused by matching boundary conditions. Thus, we open the possibility for dramatically increased measurement volumes, allowing significantly more power than a traditional cavity haloscope, especially at high frequencies. Using thin wire metamaterials as a candidate plasma, we showed that plasma haloscopes provide a plausible alternative to dielectric haloscopes in the mass region 35–400 μeV, at least. Other candidate plasmas exist, which may allow the technique to be expanded into larger parameter spaces.

*Corresponding author.
alexander.millar@fysik.su.se

[1] R. D. Peccei and H. R. Quinn, *CP* Conservation in the Presence of Instantons, Phys. Rev. Lett. **38**, 1440 (1977).

[2] S. Weinberg, A New Light Boson?, Phys. Rev. Lett. **40**, 223 (1978).

[3] F. Wilczek, Problem of Strong *P* and *T* Invariance in the Presence of Instantons, Phys. Rev. Lett. **40**, 279 (1978).

[4] D. J. E. Marsh, Axion cosmology, Phys. Rep. **643**, 1 (2016).

[5] M. Kawasaki, K. Saikawa, and T. Sekiguchi, Axion dark matter from topological defects, Phys. Rev. D **91**, 065014 (2015).

[6] A. Vaquero, J. Redondo, and J. Stadler, Early seeds of axion miniclusters, J. Cosmol. Astropart. Phys. 04 (2019) 012.

[7] V. B. Klaer and G. D. Moore, The dark-matter axion mass, J. Cosmol. Astropart. Phys. 11 (2017) 049.

[8] M. Buschmann, J. W. Foster, and B. R. Safdi, Early-Universe simulations of the cosmological axion, arXiv:1906.00967.

[9] M. Gorghetto, E. Hardy, and G. Villadoro, Axions from strings: The attractive solution, J. High Energy Phys. 07 (2018) 151.

[10] M. Kawasaki, T. Sekiguchi, M. Yamaguchi, and J. Yokoyama, Long-term dynamics of cosmological axion strings, Prog. Theor. Exp. Phys. **2018,** 091E01 (2018).

[11] P. Sikivie, Experimental Tests of the Invisible Axion, Phys. Rev. Lett. **51,** 1415 (1983); Erratum, Phys. Rev. Lett. **52,** 695(E) (1984).

[12] G. Rybka et al. (ADMX Collaboration), Direct detection searches for axion dark matter, Phys. Dark Universe **4,** 14 (2014).

[13] B. M. Brubaker et al., First Results From a Microwave Cavity Axion Search at 24 μeV, Phys. Rev. Lett. **118,** 061302 (2017).

[14] W. Chung, Launching axion experiment at CAPP/IBS in Korea, in Proceedings, 12th Patras Workshop on Axions, WIMPs and WISPs: Jeju Island, South Korea, DESY: Hamburg, Germany, 2016 (Deutsches Elektronen-Synchrotron, Hamburg, 2017), pp. 30–34, http://inspirehep.net/record/1644238/files/fulltext.pdf.

[15] D. Alesini, D. Babusci, D. Di Gioacchino, C. Gatti, G. Lamanna, and C. Ligi, The KLASH Proposal, arXiv:1707.06010.

[16] M. Goryachev, B. T. Mcallister, and M. E. Tobar, Axion detection with negatively coupled cavity arrays, Phys. Lett. A **382,** 2199 (2018).

[17] P. Sikivie, N. Sullivan, and D. B. Tanner, Proposal for Axion Dark Matter Detection Using an LC Circuit, Phys. Rev. Lett. **112,** 131301 (2014).

[18] Y. Kahn, B. R. Safdi, and J. Thaler, Broadband and Resonant Approaches to Axion Dark Matter Detection, Phys. Rev. Lett. **117,** 141801 (2016).

[19] D. Budker, P. W. Graham, M. Ledbetter, S. Rajendran, and A. Sushkov, Proposal for a Cosmic Axion Spin Precession Experiment (CASPEr), Phys. Rev. X **4,** 021030 (2014).

[20] A. Caldwell, G. Dvali, B. Majorovits, A. Millar, G. Raffelt, J. Redondo, O. Reimann, F. Simon, and F. Steffen (MADMAX Working Group Collaboration), Dielectric Haloscopes: A New Way to Detect Axion Dark Matter, Phys. Rev. Lett. **118,** 091801 (2017).

[21] A. J. Millar, G. G. Raffelt, J. Redondo, and F. D. Steffen, Dielectric haloscopes to search for axion dark matter: Theoretical foundations, J. Cosmol. Astropart. Phys. 01 (2017) 061.

[22] J. Jeong, S. Youn, S. Ahn, J. E. Kim, and Y. K. Semertzidis, Concept of multiple-cell cavity for axion dark matter search, Phys. Lett. B **777,** 412 (2018).

[23] A. A. Melcn et al., Axion searches with microwave filters: The RADES project, J. Cosmol. Astropart. Phys. 05 (2018) 040.

[24] N. V. Mikheev, G. Raffelt, and L. A. Vassilevskaya, Axion emission by magnetic field induced conversion of longitudinal plasmons, Phys. Rev. D **58,** 055008 (1998).

[25] S. Das, P. Jain, J. P. Ralston, and R. Saha, The dynamical mixing of light and pseudoscalar fields, Pramana **70,** 439 (2008).

[26] A. K. Ganguly, P. Jain, and S. Mandal, Photon and axion oscillation in a magnetized medium: A general treatment, Phys. Rev. D **79,** 115014 (2009).

[27] A. J. Millar, J. Redondo, and F. D. Steffen, Dielectric haloscopes: Sensitivity to the axion dark matter velocity, J. Cosmol. Astropart. Phys. 10 (2017) 006.

[28] L. Visinelli and H. Teras, A Kinetic Theory of Axions in Magnetized Plasmas: The Axionon, arXiv:1807.06828.

[29] H. Tercas, J. D. Rodrigues, and J. T. Mendona, Axion-Plasmon Polaritons in Strongly Magnetized Plasmas, Phys. Rev. Lett. **120,** 181803 (2018).

[30] J. T. Mendonça, J. D. Rodrigues, and H. Terças, Axion production in unstable magnetized plasmas: an active source of dark-matter, arXiv:1901.05910.

[31] P. M. Bellan, Fundamentals of Plasma Physics (Cambridge University Press, Cambridge, England, 2006).

[32] COMSOL Multiphysics v. 5.4; COMSOL AB, Stockholm, Sweden, https://www.comsol.com.

[33] G. G. Raffelt, Astrophysical axion bounds, Lect. Notes Phys. **741,** 51 (2008).

[34] J. H. Chang, R. Essig, and S. D. McDermott, Supernova 1987A constraints on sub-GeV dark sectors, millicharged particles, the QCD axion, and an axion-like particle, J. High Energy Phys. 09 (2018) 051.

[35] R. G. Mani, L. Ghenim, and J. B. Choi, Quantum coherence effects and field-induced localization in InSb, Phys. Rev. B **43,** 12630 (1991).

[36] L. Wang, X. Chen, A. Yu, Y. Zhang, J. Ding, and W. Lu, Highly sensitive and wide-band tunable terahertz response of plasma waves based on graphene field effect transistors, Sci. Rep. **4,** 5470 (2014).

[37] C. Hutter, E. A. Tholén, K. Stannigel, J. Lidmar, and D. B. Haviland, Josephson junction transmission lines as tunable artificial crystals, Phys. Rev. B **83,** 014511 (2011).

[38] J. B. Pendry, A. J. Holden, D. J. Robbins, and W. J. Stewart, Low frequency plasmons in thin-wire structures, J. Phys. Condens. Matter **10,** 4785 (1998).

[39] P. A. Belov, R. Marqués, S. I. Maslovski, I. S. Nefedov, M. Silveirinha, C. R. Simovski, and S. A. Tretyakov, Strong spatial dispersion in wire media in the very large wavelength limit, Phys. Rev. B **67,** 113103 (2003).

[40] I. G. Irastorza and J. A. Garcia, Direct detection of dark matter axions with directional sensitivity, J. Cosmol. Astropart. Phys. 10 (2012) 022.

[41] S. Knirck, A. J. Millar, C. A. J. O'Hare, J. Redondo, and F. D. Steffen, Directional axion detection, J. Cosmol. Astropart. Phys. 11 (2018) 051.

[42] M. Dine, W. Fischler, and M. Srednicki, A simple solution to the strong CP problem with a harmless axion, Phys. Lett. B **104,** 199 (1981).

[43] A. R. Zhitnitsky, On possible suppression of the axion hadron interactions, Yad. Fiz. 31, 497 (1980) [Sov. J. Nucl. Phys. **31,** 260 (1980)].

[44] L. Zhong et al. (HAYSTAC Collaboration), Results from phase 1 of the HAYSTAC microwave cavity axion experiment, Phys. Rev. D **97,** 092001 (2018).

[45] W. U. Wuensch, S. De Panfilis-Wuensch, Y. K. Semertzidis, J. T. Rogers, A. C. Melissinos, H. J. Halama, B. E. Moskowitz, A. G. Prodell, W. B. Fowler, and F. A. Nezrick, Results of a laboratory search for cosmic axions and other weakly coupled light particles, Phys. Rev. D **40,** 3153 (1989).

[46] C. Hagmann, P. Sikivie, N. S. Sullivan, and D. B. Tanner, Results from a search for cosmic axions, Phys. Rev. D **42,** 1297 (1990).

[47] S. J. Asztalos *et al.* (ADMX Collaboration), A SQUID-Based Microwave Cavity Search for Dark-Matter Axions, Phys. Rev. Lett. **104,** 041301 (2010).

[48] K. van Bibber, Status of the ADMX-HF experiment, in *Proceedings, 11th Patras workshop on axions, WIMPs and WISPs: Zaragoza, Spain, June 22-26, 2015.* (DESY: Hamburg, Germany, 2015), http://axion-wimp2015.desy .de/sites/sites_conferences/site_axion-wimp2015/content/ e13847/e16320/Proc_11thPatras.pdf.

[49] G. Carosi, Cavity-based searches for relic axions, *Proceedings of at Bethe Forum on Axions and the Low Energy Frontier* (2016), http://bctp.uni-bonn.de/bethe-forum/2016/ axions/talks/Carosi.pdf.

[50] B. T. McAllister, G. Flower, E. N. Ivanov, M. Goryachev, J. Bourhill, and M. E. Tobar, The ORGAN Experiment: An axion haloscope above 15 GHz, Phys. Dark Universe **18,** 67 (2017).

[51] N. Du *et al.* (ADMX Collaboration), A Search for Invisible Axion Dark Matter with the Axion Dark Matter Experiment, Phys. Rev. Lett. **120,** 151301 (2018).

[52] P. Brun *et al.* (MADMAX Collaboration), A new experimental approach to probe QCD axion dark matter in the mass range above 40 μeV, Eur. Phys. J. C **79,** 186 (2019).